Evolution of microstructure in stainless martensitic steel for seamless tubing

Cite as: AIP Conference Proceedings **1915**, 040048 (2017); https://doi.org/10.1063/1.5017396
Published Online: 12 December 2017

I. Yu. Pyshmintsev, S. M. Bityukov, V. I. Pastukhov, S. V. Danilov, L. O. Vedernikova, and M. L. Lobanov

Evolution of Microstructure in Stainless Martensitic Steel for Seamless Tubing

I. Yu. Pyshmintsev[1, a)], S. M. Bityukov[1, b)], V. I. Pastukhov[2], S. V. Danilov[2, c)], L. O. Vedernikova[2, d)] and M. L. Lobanov[2, e)]

[1]*RosNITI JSC, 30 Novorossiiskaya St., Chelyabinsk, 454139, Russia*
[2]*B. N. Yeltsin Ural Federal University, 19 Mira St., Ekaterinburg, 620002, Russia.*

[a)]PyshmintsevIU@tmk-group.com,
[b)]BitiukovSM@tmk-group.com
[c)]Corresponding author: s.v.danilov@bk.ru
[d)]larisa.vedernikova@urfu.ru
[e)]m.l.lobanov@urfu.ru

Abstract. Scanning electron microscopy with orientation analysis by the electron backscatter diffraction (EBSD) method is used to study microstructures and textures formed in the 0.08C-13Cr-3Ni-Mo-V-Nb steel through seamless tube production route: after hot deformation by extrusion; after quenching from various temperatures and subsequent high tempering. It is shown that the martensitic microstructure formed both after hot deformation and after quenching is characterized by the presence of deformation crystallographic texture, which is predetermined by the texture of austenite. The effect of heat treatment on texture, packet refinement, lath width, precipitation of carbides and Charpy impact energy is analyzed.

INTRODUCTION

The development of onshore and offshore oil and gas fields, with simultaneous exposure to seawater and carbon dioxide, requires high-chromium corrosion-resistant steels, such as "13Cr" and "super-chromium" [1-3]. High alloying of these materials provides fine, mainly martensitic microstructure additionally strengthened by carbide precipitations and a unique combination of corrosion and mechanical properties resulting from deformation and heat treatments [4-7]. This paper studies the peculiarities of the microstructure forming in high-chromium martensitic steel through few steps of industrial seamless pipe processing – hot deformation, quenching and tempering at high temperature – for better understanding and further optimization of technology.

RESEARCH METHODS

Specimens sized 130×70×6 mm were sampled from seamless hot-deformed tubes. This state of the low carbon 0.08C-13.5Cr-3Ni-Mo-V-Nb steel was used as initial. Hot-deformed (HD) specimens were subjected to heat treatments by the following two modes: 1) heating to 950-960 °C, holding for 15 min followed by air cooling for martensite formation (quenching, Q), tempering at 620 ± 5 °C for 45 min, QT-960; 2) after the above quenching, reheating to 870 ± 5 °C, holding for 15 min followed by air cooling and high tempering, QT-960-870. Metallographic sections were prepared in the RD-ND plane (where RD is the direction of hot deformation and ND is the direction of the normal to the surface). The microstructure was studied using a ZEISS CrossBeam AURIGA scanning microscope with accelerating voltage of 20 kV. To determine the orientation of individual grains and analyze the local texture, EBSD HKL Inca with the Oxsford Instruments analysis system was used. The texture was

Mechanics, Resource and Diagnostics of Materials and Structures (MRDMS-2017)
AIP Conf. Proc. 1915, 040048-1–040048-5; https://doi.org/10.1063/1.5017396
Published by AIP Publishing. 978-0-7354-1607-9/$30.00

studied using orientation distribution functions (ODF). After the final treatment, the samples were cut along the RD, impact bending tests in accordance with GOST 9454-78 were carried out at −60 °C. V-shaped notches were cut parallel to the tube surface. Phase thermodynamic equilibria were calculated using the ThermoCalc software.

RESULTS AND DISCUSSION

The microstructure of the samples both in HD and QT (Fig. 1) consists mainly of martensitic packets. The size of the packets for all cases is comparable to the size of the deformed (elongated parallel to RD) austenite grains (Fig. 1, a, b).

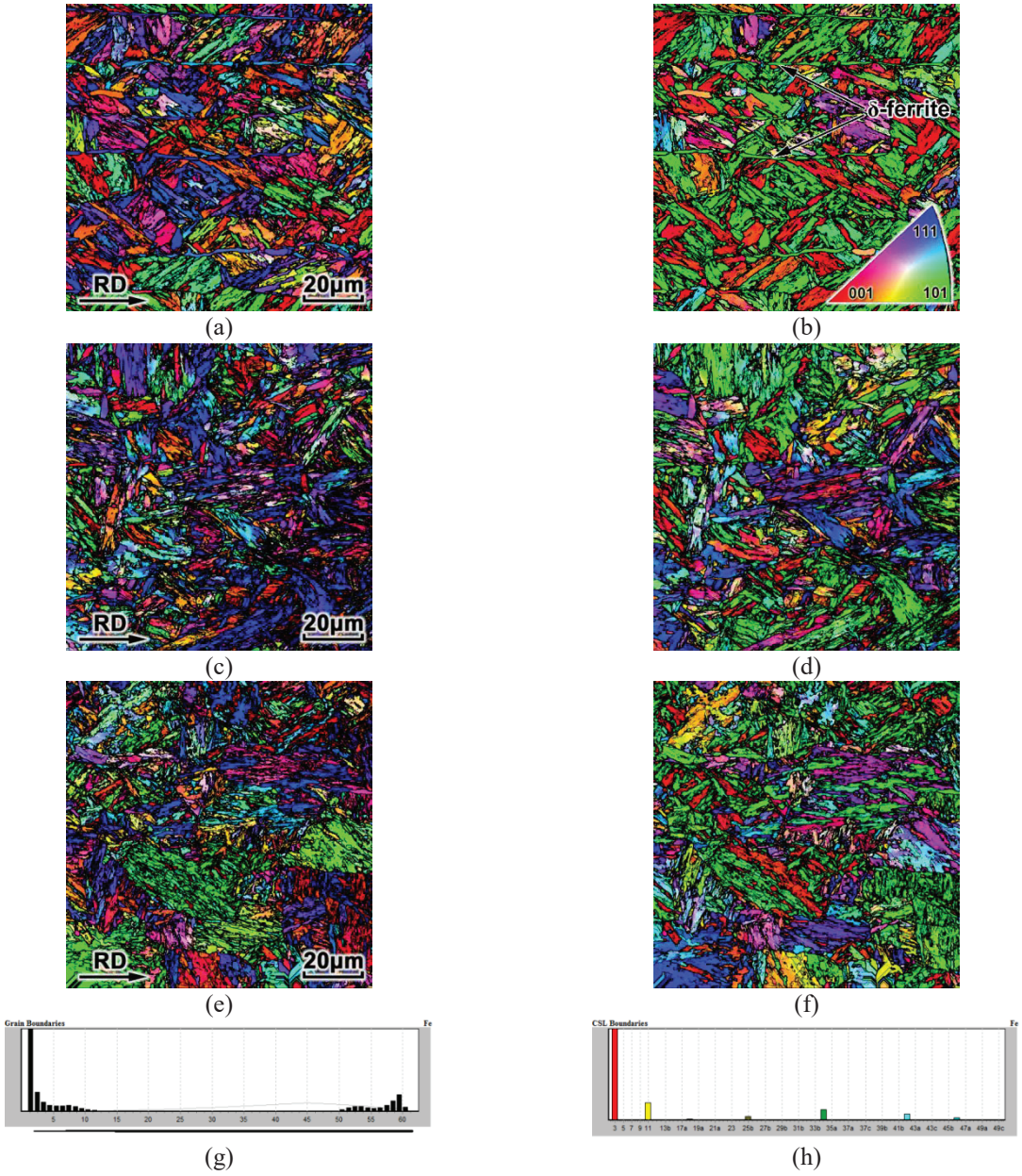

FIGURE 1. The microstructure of the steel under hot deformation and heat treatment in the form of orientation maps (EBSD): a, b – hot deformation; c, d – QT-960 state 62; e, f, g, h – QT-950-870 state; a, c, e – orientation maps from the direction normal to the tube surface; b, d, f – orientation from the cross section normal to RD; g – distribution of intercrystalline boundaries; h – distribution of CSL boundaries

The lath width and the size of martensitic packets notably decrease in the sequence HD → QT-960 → QT-960-870 (Fig. 1, a, c, e). Elongated ferrite-phase grains are observed in the samples after HD along the boundaries of the initial deformed γ-grains (Fig. 1, a, b). This ferrite can be identified as traces of the high-temperature delta-phase existing in steel after solidification. The final martensitic microstructure is characterized by the presence of well recognizable crystallographic texture consisting of the orientations {001} <110>, {013} <100> {011} <110>, {11k} <110>, {110} <110 > (Fig. 3, a, b, e, f) after all treatments. The intensity of individual orientations may vary significantly in some areas in all the states studied. However, in general, the spectrum of martensitic orientations remains the same. According to [8], the spectrum in these areas corresponds to α-phase orientations, resulting from two phase-shear transformations of strained stable-orientation austenite [9, 10] in accordance with the orientation ratios between Kurdyumov-Sachs and Nishiyama-Wassermann. The distributions of the intercrystalline and special boundaries (Fig. 1, g, h) correspond exactly to the spectra of special orientations arising from shear γ → α transformation according to [8].

The applied orientational EBSD technique has allowed us to define structurally δ-ferrite in the samples in HD (Fig. 1, a, b) and to analyze the texture (Fig. 3, c, d). All the indicated orientations of the ferrite formed at HD, namely, {001} <110>, {11k} <110>, are stable deformation orientations of the BCC lattice [9]. It should be noted that, taking into account the crystal-geometric characteristics of δ-ferrite (orientation, shape and size of grains), it can be considered as a kind of "macrodefect", which needs to be eliminated by heat treatment. The propagation of longitudinal cracks will be predetermined in the crystallographic planes {001} of elongated delta-ferrite grains [10, 11].

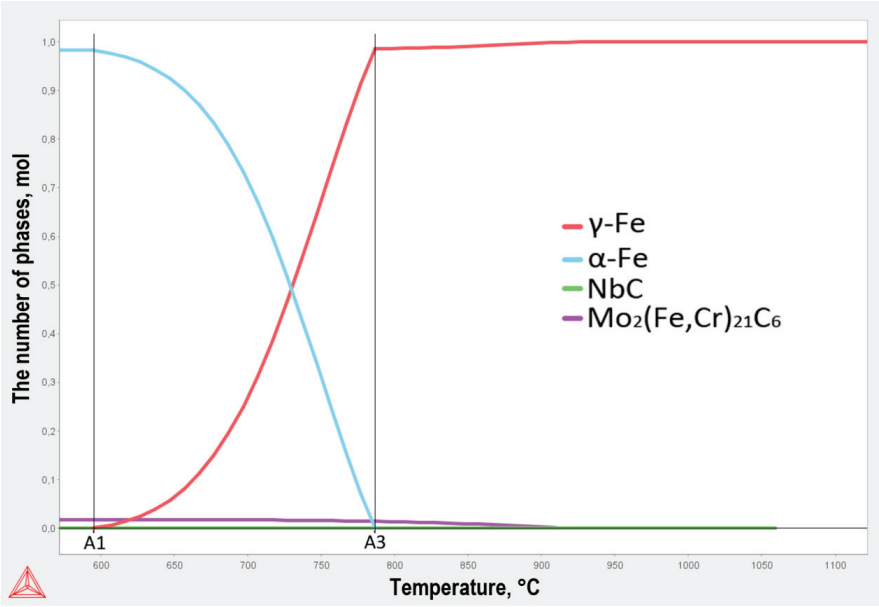

FIGURE 2. The temperature dependence of the phase composition in the studied steel resulting from calculated thermodynamic equilibrium

It is important to note that the orientations of martensite after HD and after QT are similar. This assumes realization of textural heredity in the material; the main components of the austenite texture are transformed into a discrete set of orientations of martensite upon cooling after HD. With subsequent heating, the martensite orientations are transformed into austenite texture, which in general coincides with the γ-phase texture in the HD state. Quenching of overcooled austenite leads to the formation of martensite with its inherent set of texture components, and so on. A similar mechanism of texture evolution during phase transformations [12] assumes that there are some factors responsible for heredity in the structure of the material after HD. According to [10, 13], the reasons may be special boundaries Σ3 and Σ11 between the deformed austenite grains formed due to hot deformation, the relative arrangement of which in the material structure is additionally pinned by precipitates of carbide phases.

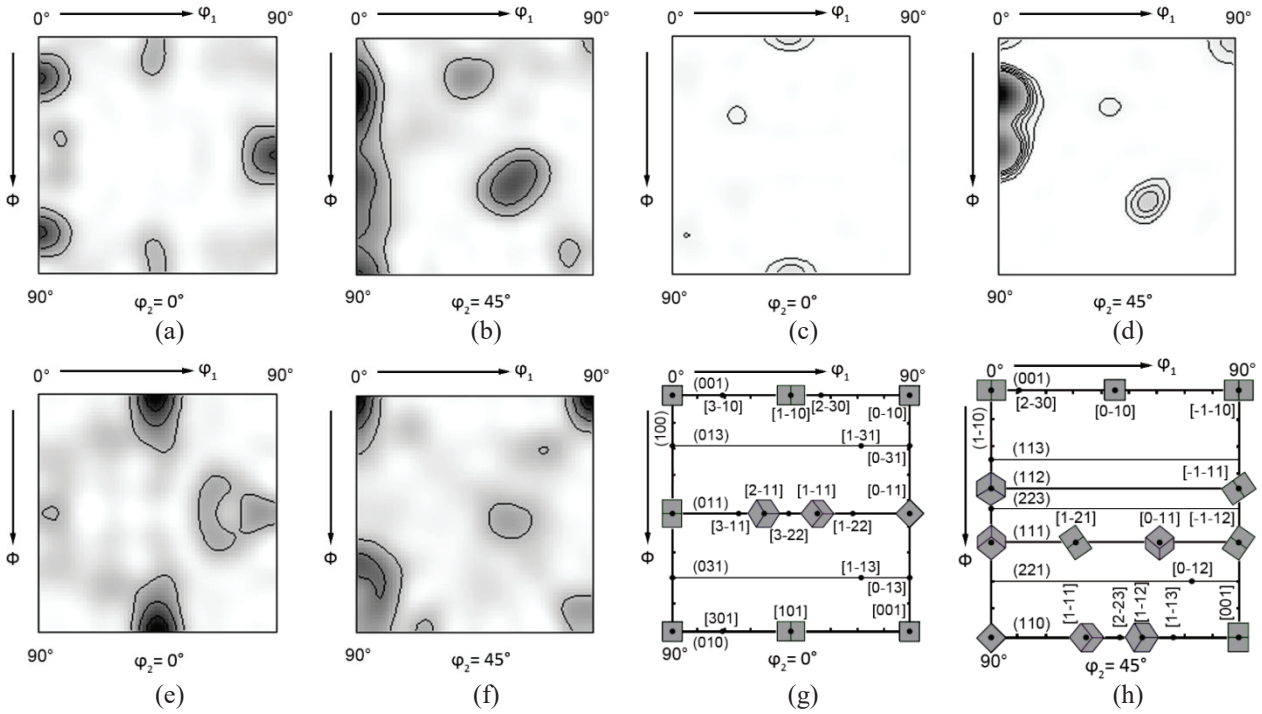

FIGURE 3. The texture of the steel in the HD (a-d) and QT-960-870 (e, f) states as ODF sections: c,d – sections for δ–ferrite grains; g, h – schematic orientations from the direction perpendicular to the RD-ND plane

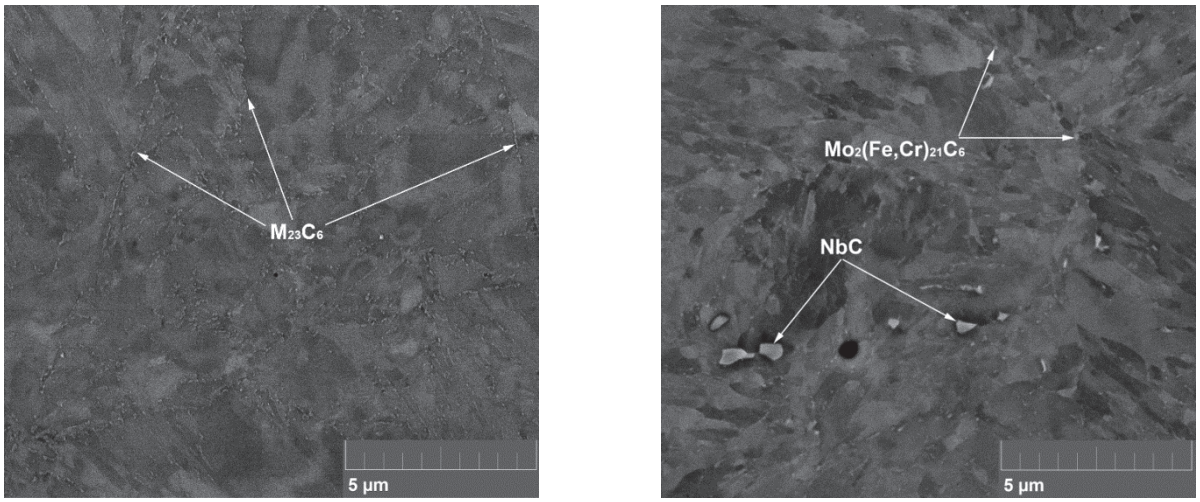

(a) (b)

FIGURE 4. The microstructure of the steel in the heat treated states (image in backscattered electrons): a – QT-960; b – QT-960-870

The study of carbide phases (Fig. 4) and the calculations of thermodynamic phase equilibria (Fig. 2) suggest that carbide precipitation occurs in two stages. Comparatively large NbC particles (Fig. 4, b) are formed in the HD stage on the boundaries of austenite grains, preventing their recrystallization. Fine $M_{23}C_6$-type carbide particles precipitate between the martensite lathes during tempering (Fig. 4, a). The second quenching results in the formation of larger $Mo_2(Fe,Cr)21C_6$ particles at 870 °C predominately on the γ-phase boundaries, thereby reducing the amount of the fine carbide phase formed under high-temperature tempering (Fig. 4, b).

It is demonstrated that double quenching and tempering (QT-960-870) leads to higher values of low-temperature specific Charpy energy KCV-60 in comparison with QT-960: 99±3 J/cm^2 against 87±4 J/cm^2, respectively. Apparently, this is mainly due to the fine microstructure of the martensitic packets. Despite the lower portion of fine carbides in the microstructure after double heat treatment, the strength parameters are similar in both the QT-960 and QT-960-870 states.

TABLE 1. Strength parameters

State	Tensile strength, MPa	Yield strength, MPa	KCV-60, J/cm^2
QT-960	970	863	87
QT-960-870	958	868	99

CONCLUSION

Thus, the study has shown the possibilities of varying the structure of a high-chromium martensitic steel due to the parameters of deformations and thermal treatments for optimizing the production technology or manufacturing products with a required combination of mechanical properties.

ACKNOWLEDGMENTS

The work was done using the equipment of the laboratory of Structural Methods of Analysis and Properties of materials and nanomaterials of the Collective Use Center affiliated to Ural Federal University. The study was supported by the program of increasing the competitiveness of the leading Russian universities, RF Government resolution No. 211, contract No. 02.A03.21.0006. We are grateful to the TMK company for their support and assistance in organizing the study.

REFERENCES

1. H. Asahi, H. Inoue, K. Nose, N. Ayukawa, T. Muraki, H. Tamehiro and M. Oka, Nippon Steel Technical Report 53–58 (1997).
2. T. G. Gooch, Welding Journal **74**, 213–223 (1995).
3. P. R. Rhodes, Corrosion **57**, 923–966 (2001).
4. K. H. Lo, C. H. Shek, and J. K. L. Lai, Materials Science and Engineering R: Reports **65**, 39–104 (2009).
5. M. V. Odnobokova, A. Y. Kipelova, A. N. Belyakov and R. O. Kaibyshev, Physics of Metals and Metallography **117**, 390–398 (2016).
6. Y. Y. Song, D. H. Ping, F. X. Yin, X. Y Li and Y. Y. Li, Materials Science and Engineering A **527**, 614–618 (2010).
7. M. Akhmedyanov, S. V. Rushchits, and M. A. Smirnov, "Hot deformation of martensitic and supermartensitic stainless steels" in International Conference on Industrial Engineering-2016, Materials Science Forum 870 (Trans Tech Publications, Switzerland, 2016), 259–264.
8. M. L. Lobanov, G. M. Rusakov, A. A. Redikultsev, S. V. Belikov, M. S. Karabanalov, E. R. Struina and A. M. Gervasyev, Physics of Metals and Metallography **117**, 254–259 (2016).
9. M. Hölscher, D. Raabe, and K. Lücke, Acta Metallurgica Et Materialia **42**, 879–886 (1994).
10. I. Yu. Pyshmintsev, A. O. Struin, A. M. Gervasyev, M. L. Lobanov, G. M. Rusakov, S. V. Danilov and A. B. Arabey, Metallurgist 1–8 (2016).
11. I. Yu. Pyshmintsev, I. N. Veselov, A. A. Yakovleva, M. L. Lobanov and S. V. Danilov, "Evolution of the texture of low-carbon microalloyed pipe steel in the seamless pipe manufacturing process," in 10th International Conference on Mechanics, Resource and Diagnostics of Materials and Structures, MRDMS 2016, AIP Conference Proceedings 1785 (American Institute of Physics, Melville, NY, 2016), 040053.
12. S. V. Danilov, E. R. Struina and M. D. Borodina, Steel in Translation **47**, 188–189 (2017).
13. M. L. Lobanov, S. V. Danilov, A. O. Struin, M. D. Borodina and I. Yu. Pyshmintsev, Bulletin of the South Ural State University. Ser. Metallurgy **16**, 46–54. (2016) (in Russ.).